Identification of the *Phytophthora* PAMP Pep-13 Receptor Using Diploid Potato Inbred Lines

Xuefeng Fan[1#], Dongyue Li[1#], Lin Cheng[2#], Yuqi Zhu[1,3], Yue Han[1], Chunzhi Zhang[4], Sanwen Huang[2], Tongjun Sun[1*].

[1] Shenzhen Branch, Guangdong Laboratory for Lingnan Modern Agriculture, Genome Analysis Laboratory of the Ministry of Agriculture and Rural Affairs, Agricultural Genomics Institute at Shenzhen, Chinese Academy of Agricultural Sciences, Shenzhen, China.

[2] National Key Laboratory of Tropical Crop Breeding, Shenzhen Branch, Guangdong Laboratory of Lingnan Modern Agriculture, Genome Analysis Laboratory of the Ministry of Agriculture and Rural Affairs, Agricultural Genomics Institute at Shenzhen, Chinese Academy of Agricultural Sciences, Shenzhen, China.

[3] State Key Laboratory of Crop Stress Adaptation and Improvement, The Zhongzhou Laboratory for Integrative Biology, School of Life Sciences, Henan University, Kaifeng, China.

[4] State Key Laboratory of Genome and Multi-omics Technologies，Shenzhen Branch, Guangdong Laboratory of Lingnan Modern Agriculture, Key Laboratory of Synthetic Biology, Ministry of Agriculture and Rural Affairs, Agricultural Genomics Institute at Shenzhen, Chinese Academy of Agricultural Sciences, Shenzhen, China.

[#] Contributed equally.

* Correspondence: Tongjun Sun (suntongjun@caas.cn).

ABSTRACT

Plants employ cell surface receptors to recognize pathogen-associated molecular patterns (PAMPs) and activate pattern-triggered immunity, a crucial defense mechanism against invading pathogens. Pep-13 is a PAMP derived from a class of conserved cell wall transglutaminases present in *Phytophthora* species, and its receptor PERU was reported recently. In our parallel study, we observed distinct responses to Pep-13 between two diploid potato inbred lines: E454 recognizes Pep-13, whereas A018 does not. Genetic analysis demonstrated that Pep-13 recognition in E454 is controlled by a single genetic locus, tentatively designated *TGER* (*Transglutaminase elicitor response*). Through bulked segregant analysis sequencing, followed by complementation assays, we found that the *TGERa* gene in E454 is essential for Pep-13 recognition. Sequence alignment revealed that TGERa shares 99.91% amino acid sequence identity with PERU, indicating that *TGERa* and *PERU* are allelic variants of the same gene (*PERU*/*TGERa*). *TGERb*, a highly homologous gene of *TGERa*, was identified in the E454 genome; notably, TGERa, but not TGERb, can recognize Pep-13. We further demonstrated that TGERb exhibits defects in both ligand binding and association with the co-receptor StSERK3A. Additionally, we found that the *TGERa* allele in A018 is a weak allele with reduced expression levels, presumably resulting from a 3 kb DNA fragment insertion in its first intron. Heterologous introduction of *TGERa* into *Nicotiana benthamiana* and tomato significantly enhanced their resistance to *Phytophthora infestans*. Collectively, our findings confirm that PERU/TGERa functions as the Pep-13 receptor in potato and provide a valuable molecular target for improving *Phytophthora* resistance in plants.

Keywords: Potato; *Phytophthora infestans*; Pep-13; Pattern Recognition Receptor (PRR); PERU/TGERa.

54 **INTRODUCTION**

55 Potato (*Solanum tuberosum* L.), the most important tuber crop, is a staple food
56 for approximately 1.3 billion people globally (Stokstad, 2019). Cultivated
57 potatoes are primarily propagated asexually via tubers, and the complexity of
58 their tetraploid genome results in a prolonged breeding cycle. To address this
59 challenge, a diploid potato hybrid breeding project was launched based on
60 diploid potato inbred lines (Zhang et al., 2021; Cheng et al., 2025), which not
61 only accelerates the potato breeding process but also provides materials and
62 genomic data resources for researches on potato functional genomics.

63 Late blight, caused by *Phytophthora infestans*, is a devastating disease
64 affecting potato yield (Nowicki et al., 2012), and harnessing the plant's own
65 immune receptors provides a sustainable and eco-friendly solution for late
66 blight control. Specifically, pattern recognition receptors (PRRs) localized on
67 the plant cell surface recognize pathogen-associated molecular patterns
68 (PAMPs), thereby initiating pattern-triggered immunity that restricts pathogen
69 invasion (Jones and Dangl, 2006; Zhou and Zhang, 2020). A few well-studied
70 PAMPs have been reported in the genus *Phytophthora*, such as INF1, nlp20,
71 and XEG1, which are specifically recognized by ELR (Du et al., 2015) and
72 NbREL (Chen et al., 2023a), *Arabidopsis* RLP23 (Albert et al., 2015), and
73 NbRXEG1 (Wang et al., 2018), respectively. Notably, heterologous expression
74 of such PRRs confers enhanced disease resistance in plants (Albert et al.,
75 2015; Chen et al., 2023a).

76 Pep-13 is a 13-amino-acid peptide derived from a class of cell wall
77 transglutaminases (TGase) in the genus *Phytophthora*, and Pep-25 is a
78 25-amino-acid peptide that contains the Pep-13 sequence (Nürnberger et al.,
79 1994). Both peptides share similar activity: certain potato cultivars can
80 recognize Pep-13/25, initiating immune responses including MAPK activation,
81 ROS burst, upregulation of defence genes, and the induction of hypersensitive
82 cell death (Nürnberger et al., 1994; Brunner et al., 2002). However, the
83 receptor for Pep-13 remained unknown for a long time until recently. PERU

84 (Pep-13 receptor unit), a typical leucine-rich repeat receptor kinase (LRR-RK),
85 was identified as the receptor of Pep-13 from potato *cv.* DM (Torres Ascurra et
86 al., 2023). Interestingly, PERU from accession LPH680-5 ($PERU^{LPH}$) was
87 shown to have a broad recognition ability that perceives Pep-13/25 and
88 Pep-25 variants, such as Pep-25W2A (Torres Ascurra et al., 2023).
89 In our parallel study, we explored the Pep-13-triggered response in the inbred
90 lines A6-10 (also known as A018), A6-26 (also known as A157) and E4-63
91 (also known as E454), which are the parent lines for hybrid potatoes (Zhang et
92 al., 2021). We found that Pep-13 triggered hypersensitive cell death in A157,
93 E454 and Hybrid 2 (a F_1 progeny of a cross between A018 and E454), but not
94 in A018 (Supplemental Figure 1A). Meanwhile, the F_2 population derived from
95 self-pollinated Hybrid 2 showed phenotypic segregation in response to Pep-13,
96 with the ratio of Pep-13-responsive (HR) plants to non-responsive (non-HR)
97 plants being approximately 3:1 (Supplemental Figure 1B); this result indicates
98 that Pep-13 recognition in E454 is controlled by a single genetic locus, which
99 we tentatively designated *TGER* (*Transglutaminase elicitor response*).
100 However, conflicting with this finding, the research on PERU indicated that
101 there are no PERU homologs in A6-26 and E4-63 (See Supplemental data_s4
102 of Torres Ascurra et al., 2023), creating a critical knowledge gap that this study
103 aimed to address.
104 In this study, we identified that *TGERa* in E454 is essential for Pep-13
105 recognition. Sequence alignment revealed that TGERa shares 99.91% amino
106 acid identity with PERU, indicating that *TGERa* and *PERU* are the same gene
107 (designated as *PERU*/*TGERa*; for simplicity, *TGERa* is used hereafter). We
108 further identified *TGERb*, a highly homologous gene of *TGERa* in the E454
109 genome, which cannot recognize Pep-13. Additionally, we found that the
110 *TGERa* allele in A018 is a weak allele with reduced expression. Lastly, we
111 showed that introduction of *TGERa* into plants significantly enhanced their
112 resistance to *Phytophthora* pathogens, highlighting the potential of *TGERa* as
113 a valuable molecular target for improving *Phytophthora* resistance in crops.

RESULTS AND DISCUSSION

Differential responses of potato inbred lines A018, A157 and E454 to Pep-13

To identify the receptor responsible for Pep-13 perception using potato inbred lines generated by the Upotato project (Zhang et al., 2021), we first evaluated their responses to Pep-13. As shown in Figure 1A, A157 and E454 exhibited hypersensitive response (HR) cell death to Pep-13 but not to the nearly inactive Pep-13W2A variant (Brunner et al., 2002). Unexpectedly, Pep-13 failed to trigger cell death in A018, although A018 and A157 are homozygous inbred lines derived from the same ancestral parent, PG6359 (Zhang et al., 2021). Additionally, Désirée, but not the Atlantic, exhibited cell necrosis upon Pep-13 treatment (Figure 1A). Consistent with the HR phenotypes, Pep-13 treatment activated MAPK signaling in A157 but not in A018 (Figure 1B and 1C). Notably, four Pep-13-responsive genes (Nietzschmann et al., 2019), namely *StTHT*, *StPALs*, *StFAD*, and *St4-CL*, were strongly induced in A157, but showed little or no induction in A018 (Figure 1D). Collectively, these results demonstrate distinct responses of potato lines to Pep-13, with A018 showing a unique pattern of no cell death but weak induction of some Pep-13-responsive genes.

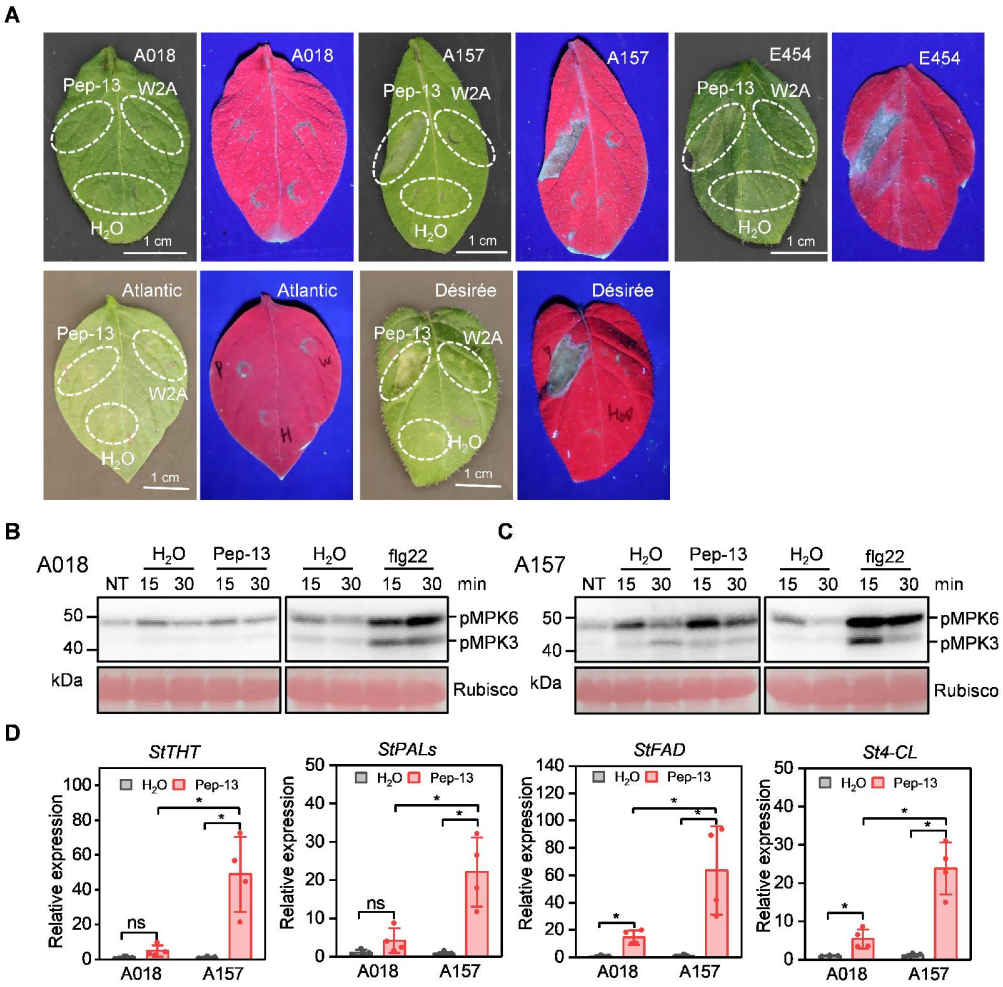

Figure 1. Differential responses of potato inbred lines A018, A157, E454 and cultivars Atlantic and Désirée to Pep-13.

(A) Differential responses of potato cultivars to Pep-13. Leaves were infiltrated with 100 μM Pep-13, Pep-13W2A (a Pep-13 variant) and H_2O. Photos were taken under natural light (green leaf) and UV light (red fluorescence) at 24 h post-infiltration. Bar = 1 cm.

(B-C) Pep-13-induces MAPK activation in A157 but not in A018. Leaves of A018 **(B)** and A157 **(C)** were sprayed with 100 μM Pep-13 or H_2O. Samples were collected at 15 and 30 min post-treatment, and MAPK activation was detected by western blot using an anti-p44/42-ERK antibody. flg22 (5 μM) served as a positive control, and non-treated (NT) leaves served as a negative control.

(D) Pep-13-responsive genes are strongly induced in A157 but show little or no induction in A018. Transcript levels of *StTHT*, *StPALs*, *StFAD*, and *St4-CL* were analyzed by RT-qPCR in leaves of A018 and A157 at 4 h after infiltration with 100 μM Pep-13 or H_2O. *NbEF1α* used as reference gene. Data represent mean ± s.d. n = 4. Asterisks indicate statistically significant differences (*$p < 0.05$, Student's t-test); ns, no significant diference.

Genetic mapping of *TGERa* and validation

Using bulked segregant sequencing, we identified that the *TGER* locus is located within the chr 0-3 Mb region of the E454 genome, which was further

152 narrowed down to 24 candidate genes (see details in Supplemental Note 1).
153 We successfully cloned 21 of these candidate genes and screened their
154 responsiveness to Pep-13 via *Agrobacterium*-mediated transient expression in
155 *N. benthamiana* (*Nb*) leaves. The gene expressed by construct #9 was found
156 to respond to Pep-13 (Supplemental Figure 2), which was designated as
157 *TGERa*. Next, we generated transgenic *Nb* lines expressing *TGERa* under its
158 native promoter (*np-TGERa Nb* lines); these transgenic lines exhibited cell
159 death in response to Pep-25 but showed no or weak cell death to Pep-13
160 treatment (Supplemental Figure 3A). However, both Pep-13 and Pep-25 were
161 able to induce MAPK activation in *np-TGERa Nb* lines; furthermore, Pep-13
162 treatment of these transgenic plants significantly activated the expression of
163 *NbACRE31* and *NbCYP71D20* (Supplemental Figure 3B and 3C). These
164 results indicate that *TGERa* is responsive to both Pep-13 and Pep-25, with
165 Pep-25 exhibiting stronger activity in inducing cell death than Pep-13 under
166 conditions of low TGERa protein levels. Stable expression of *TGERa* in cv.
167 MicroTOM and potato Atlantic conferred the ability to recognize Pep-13 and
168 Pep-25, leading to the induction of cell death (Supplemental Figure 3D-3G).
169 Collectively, these findings demonstrated that TGERa is responsive to
170 Pep-13/25.

171 **Immune-related SERKs are required for Pep-13 perception**

172 TGERa is a typical leucine-rich repeat receptor kinase (LRR-RK). To identify its
173 interacting proteins, immunoprecipitation-mass spectrometry (IP-MS) was
174 performed in *N.benthamiana* (*Nb*) leaves, revealing six NbSERK proteins,
175 including NbSERK3A, NbSERK3B, NbBAK1a, NbBAK1b, NbSERK2a, and
176 NbSERK2b, as Pep-13-induced interacting partners of TGERa (Supplemental
177 Figure 4A). Phylogenetic analysis showed that these six NbSERK proteins,
178 together with their potato homologs (StSERK2, StSERK3A, and StSERK3B)
179 and *Arabidopsis* SERKs (Ma et al., 2016; Li et al., 2025), form a single clade
180 (Supplemental Figure 4B). Given the evolutionary conservation of these SERK
181 proteins and their known roles in plant immunity, we further confirmed that

182 Pep-13 induces the interaction between TGERa and three StSERKs
183 (Supplemental Figure 5A-5C). Additionally, silencing of these six *NbSERK*
184 genes in *Nb* leaves blocked Pep-25/TGERa-induced cell death (Supplemental
185 Figure 5D-5J). Notably, we showed that TGERa can bind to biotin-labeled
186 Pep-13 (Supplemental Figure 5L). Collectively, these results demonstrate that
187 TGERa forms a receptor complex with immune-related SERKs to mediate the
188 perception of Pep-13.

189 **Comparison of coding sequences between TGERa and PERU**

190 Sequence analysis revealed that the coding sequence (CDS) of TGERa^{E454} is
191 78 bp longer than that of PERU^{DM}, which corresponds to an in-frame upstream
192 open reading frame (uORF) (Supplemental Figure 6A). This observation
193 indicates that the predicted TGERa^{E454} contains an additional 26 amino acids
194 at the N-terminus compared to PERU^{DM}; whereas the remaining protein
195 sequence is nearly identical between the two, with only a single amino acid
196 substitution (A317 in PERU vs. G317 in TGERa-dN26), confirming that
197 TGERa^{E454} and PERU^{DM} are allelic variants of the same gene.

198 To determine the translational start site of TGERa^{E454}, we individually mutated
199 the ATG codons of uORF1 and the main ORF. Mutation of the main ORF ATG,
200 which restricts protein translation to uORF1, significantly reduced TGERa^{E454}
201 protein accumulation irrespective of being driven by 35S or its native
202 promoters (Supplemental Figure 6B-6E). These findings indicate that
203 TGERa^{E454} protein translation primarily initiates from the main ATG. Given that
204 TGERa is a single-pass transmembrane protein, the additional 26-amino-acid
205 sequence at the N-terminus may impair its signal peptide function and disrupt
206 normal translation processes, thereby reducing TGERa^{E454} protein levels.

207 In contrast, the annotated PERU protein from LPH60-5 (PERU^{LPH}) contains an
208 extra 24-amino-acid sequence between residues T372 and G373 compared to
209 TGERa/PERU, which is encoded by an in-frame intron 2 (Supplemental Figure
210 7A and 7B). Further analysis demonstrated that this intron 2 retention occurs in
211 a subset of *TGERa* transcripts extracted from A157 leaves, both under normal

212 conditions and following *Phytophthora* inoculation (Supplemental Figure 7C
213 and 7D). To characterize the function of the protein translated from transcripts
214 with intron 2 retention, we introduced synonymous mutations into this intron 2
215 to generate *TGERa-In2R*, which abolishes intron 2 splicing while preserving
216 the encoded sequence as the extra 24 amino acids in $PERU^{LPH}$ (Supplemental
217 Figure 7E and 7F). Functional assays showed that, in contrast to TGERa,
218 TGERa-In2R failed to activate MAPK or induce cell death following Pep-13
219 treatment (Supplemental Figure 8A and 8B) and was unable to bind Pep-13 or
220 Pep-25 (Supplemental Figure 8C and 8D). These results demonstrate that the
221 protein translated from transcripts with the intron 2 retention is non-functional.
222 Therefore, the additional sequence in $PERU^{LPH}$ is likely attributable to
223 annotation errors and is unrelated to its broad ligand recognition ability.

224 **TGERa/PERU, but not its close homolog TGERb, recognizes Pep-13**

225 Sequence alignment between the gene present in construct #9 and the target
226 gene *E454_03G001350.1* revealed multiple single nucleotide polymorphisms
227 (SNPs) and one insertion/deletion (indel) (Supplemental Table 3). A sequence
228 identical to *E454_03G001350.1* was subsequently re-isolated from the
229 amplification products using the same primers for *E454_03G001350.1* and
230 designated as *TGERb*. Transient expression of *TGERa* ,but not *TGERb*, in
231 *N.benthamiana* (*Nb*) leaves triggered MAPK activation and cell death following
232 Pep-13 treatment (Supplemental Figure 9A and 9B). Consistently, Pep-25
233 treatment induced cell death in transgenic *Nb* lines expressing *TGERa* but not
234 in lines expressing *TGERb* (Figure 2A). In addition, *np-TGERb Nb* lines failed
235 to elicit reactive oxygen species (ROS) burst or MAPK activation following
236 Pep-13 treatment (Figure 2B, 2C, and Supplemental Figure 9C). Further
237 biochemical analyses showed that Pep-13 treatment did not promote the
238 interaction between *TGERb* and StSERK3A (Figure 2D). In contrast to TGERa,
239 TGERb was unable to bind either Pep-13 or Pep-25 (Figure 2E and 2F).
240 Collectively, these results demonstrated that TGERb can not recognize Pep-13
241 or Pep-25, highlighting a functional divergence between the two highly

homologous proteins.

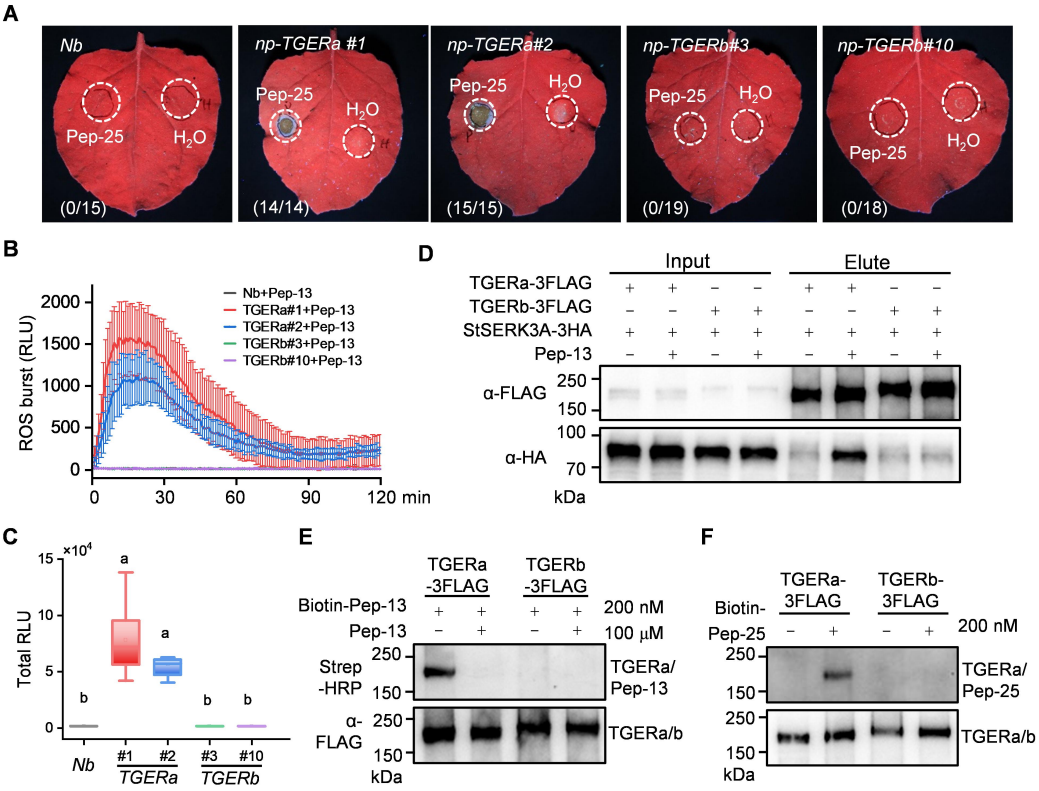

Figure 2. TGERa/PERU, but not its close homolog TGERb, recognizes Pep-13.

(A) Pep-25-induced cell death in transgenic *N. benthamiana* (*Nb*) lines expressing *TGERa* but not *TGERb.* Leaves of transgenic lines *np-TGERa* #1, *np-TGERa* #2, *np-TGERb* #3, and *np-TGERb* #10 (driven by their native promoters) were infiltrated with 100 μM Pep-25. *Nb* plants served as a negative control. Photographs were taken under UV light 5 days after infiltration.

(B-C) Pep-13-induced ROS burst in transgenic lines *np-TGERa* #1 and #2, but not in transgenic lines *np-TGERb* #3 and #10, as shown by the ROS burst curves **(B)** and total ROS production **(C)** induced by 100 nM Pep-13. Data was analyzed by two-way ANOVA followed by Tukey's multiple comparison test. Different letters indicate significant differences ($p < 0.05$, n = 8).

(D) TGERa, but not TGERb, associates with the co-receptor StSERK3A upon Pep-13 treatment. *TGERa-3Flag* or *TGERb-3Flag* was transiently co-expressed with *StSERK3A-3HA* in *Nb* leaves mediated by *Agrobacterium*. After 24 h, leaves were infiltrated with 100 μM Pep-13 or H_2O. Samples were collected 15 min post-infiltration, and TGERa/b-3Flag proteins were enriched using M2 beads. IP eluates were analyzed by western blot using anti-Flag and anti-HA antibodies.

(E-F) TGERa, but not TGERb, binds biotin-labeled Pep-13 **(E)** and Pep-25 **(F)**. *TGERa-3Flag* and *TGERb-3Flag* were transiently expressed in *Nb* leaves for 24 h. Leaves were co-infiltrated with 200 nM biotin-Pep-13/25 and 3 mM EGS, then incubated for 30 min at room temperature. Excess unlabeled Pep-13 (100 μM) was included as a competitor. TGERa/b-3Flag proteins were enriched using M2 beads, and IP eluates were detected by western blot using an anti-Flag antibody and Strep-HRP.

267

268 **TGERb exhibits defects in both ligand binding and association with**
269 **StSERK3A**

270 Protein sequence analysis revealed that the differences between TGERa and
271 TGERb are primarily inside their ectodomains, which share 85.3% sequence
272 identity (Supplemental Figure 9D). Domain swapping experiments further
273 confirmed that divergence in the ectodomain is responsible for the inability of
274 TGERb to perceive Pep-13 (Supplemental Figure 9E and 9F).

275 The ectodomain of TGERa contains 27 leucine-rich repeats (LRRs), whereas
276 TGERb harbors an additional 24-amino acid insertion in the region
277 corresponding to LRR24 of TGERa, resulting in a total of 28 LRRs. A TGERa
278 variant carrying this additional sequence (TGERa^{b24aa}) retained the ability to
279 recognize Pep-13 (Supplemental Figure 9G and 9H), indicating that this extra
280 peptide does not affect TGERa function.

281 To elucidate the mechanism underlying TGERb's inability to recognize pep-13,
282 we first performed in silico LRR substitution and predicted the interface
283 predicted TM-score (ipTM) values between chimeric TGERa variants and
284 Pep-13 using AlphaFold3 (Supplemental Table 4). Bsed on these predictions,
285 six LRRs from TGERb (LRR5/7/9/10/17/21) were selected for function analysis.
286 Among them, LRR5, LRR7, LRR9, and LRR10 were predicted to contribute to
287 Pep-13 binding, whereas LRR17 and LRR21 were hypothesized to modulate
288 interactions with SERKs. Each of these LRRs was individually substituted into
289 TGERa (Figure 3A). Functional assays revealed that TGERa^{LRR5b} and
290 TGERa^{LRR7b} exhibited impairment in Pep-13-induced cell death and ROS burst,
291 whereas TGERa^{LRR9b}, TGERa^{LRR10b}, and TGERa^{LRR17b} completely lost
292 responsiveness to Pep-13. In contrast, TGERa^{LRR21b} retained normal Pep-13
293 responsiveness (Figure 3B and 3C). Ligand-binding assays further showed
294 that TGERa^{LRR5b} and TGERa^{LRR7b} had reduced Pep-13 binding capacity, while
295 TGERa^{LRR9b} and TGERa^{LRR10b} failed to bind Pep-13. Surprisingly, TGERa^{LRR17b},
296 similar to TGERa^{LRR21b}, retained the ability to bind Pep-13 (Figure 3D).

297 Given that TGERa^{LRR17b} retained Pep-13 binding but failed to trigger immune
298 responses, we next examined its interaction with StSERK3A. TGERa^{LRR9b} and
299 TGERa^{LRR10b} - both unable to bind Pep-13 - exhibited impaired interaction with
300 StSERK3A, consistent with the observation that Pep-13 enhances the
301 interaction between TGERa and StSERK3A. In contrast, Pep-13 failed to
302 induce the interaction between TGERa^{LRR17b} and StSERK3A (Figure 3E).
303 These results demonstrate that TGERb fails to perceive Pep-13 due to defects
304 in both ligand binding and ligand-induced association with StSERK3A.

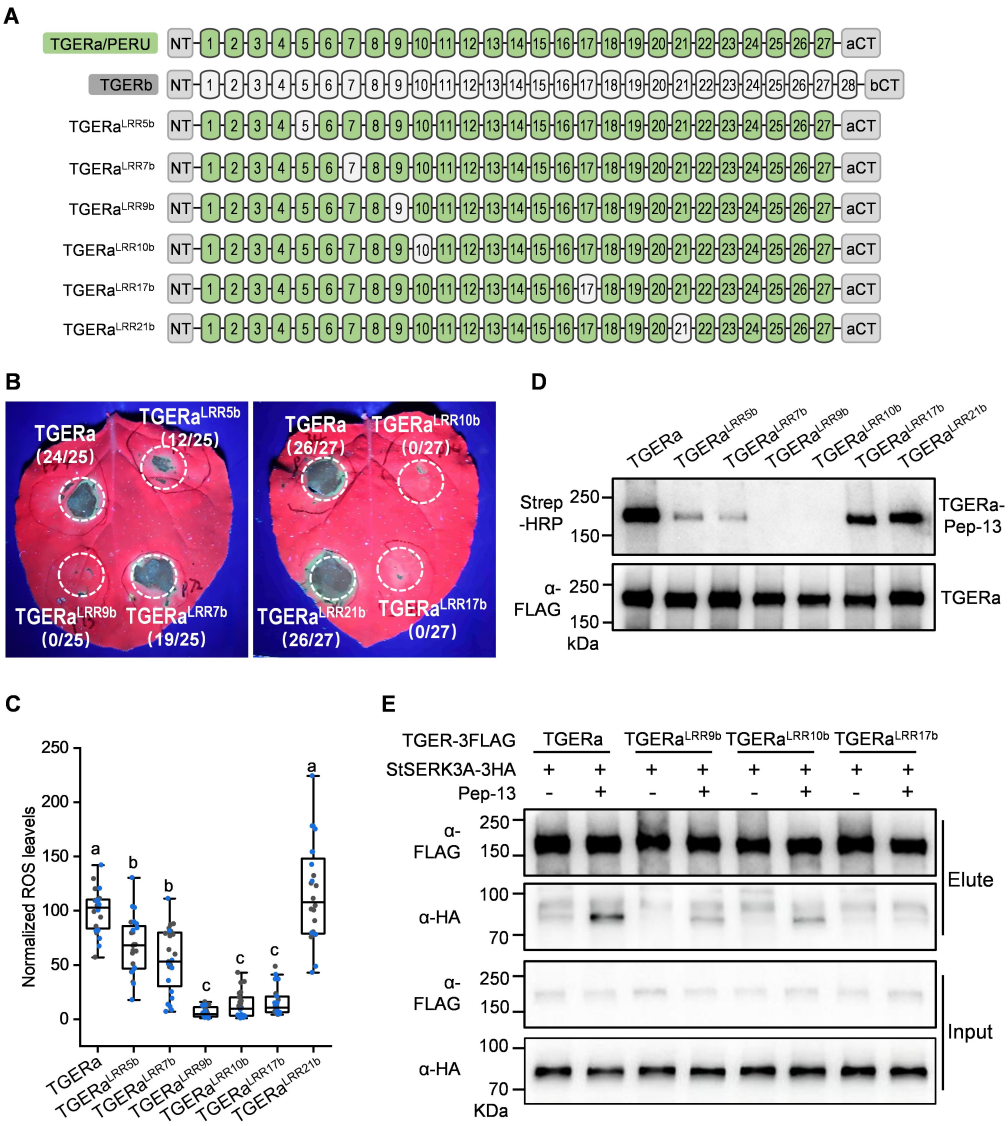

305

306 **Figure 3. Identification of TGERb's defects in Pep-13 perception.**
307 **(A)** Schematic representation of leucine-rich repeat (LRR) domain swapping between TGERa
308 and TGERb. The ectodomain of TGERa contains 27 LRRs, whereas TGERb has an additional

24-amino acid peptide in the region corresponding to LRR24 of TGERa, resulting in 28 LRRs. Indicated LRR regions of TGERb were swapped into the TGERa backbone.

(B-C) Pep-13-triggered cell death **(B)** and ROS burst **(C)** in *N. benthamiana* (*Nb*) leaves expressing wild-type *TGERa* and chimeric variants carrying the indicated TGERb LRR regions (*TGERa*^{LRRxb}). *TGERa-3Flag* and *TGERa*^{LRRxb}*-3Flag* were transiently expressed in *Nb* leaves for 24 h. For cell death assays, leaves were infiltrated with 100 μM Pep-13, and photos were taken under UV light at 48 h post-infiltration. Numbers in parentheses show the count of necrotic spots versus total spots. For ROS assays, 50 nM Pep-13 was used. The peak value of each ROS curve was normalized to that of TGERa, and analyzed by two-way ANOVA followed by Tukey's multiple comparison test. Different letters indicate significant differences ($p < 0.05$, n = 24 from two independent replicates).

(D) Differential binding of TGERa and chimeric TGERa^{LRRxb} proteins to biotin-Pep-13. *TGERa-3Flag* and *TGERa*^{LRRxb}*-3Flag* were transiently expressed in *Nb* leaves for 24 h. Leaves were co-infiltrated with 200 nM biotin-Pep-13 and 3 mM EGS, then incubated for 30 min at room temperature. Proteins were enriched using M2 beads, and eluates were detected by western blot using anti-Flag antibody and Strep-HRP.

(E) TGERa, but not TGERa^{LRR17b}, associates with the co-receptor StSERK3A upon Pep-13 treatment. *TGERa-3Flag* and *TGERa*^{LRRXb}*-3Flag* was transiently co-expressed with *StSERK3A-3HA* in *Nb* leaves. After 24 h, leaves were infiltrated with 100 μM Pep-13 or H_2O. Samples were collected 15 min post-infiltration, and proteins were enriched using M2 beads. IP eluates were analyzed by western blot using anti-Flag and anti-HA antibodies.

TGERa^{A018} represents a weak allele with reduced expression levels

To investigate the genetic basis underlying the lack of Pep-13 responsiveness in A018, we first examined the genomic organization of TGER loci in diploid potato lines. Using the ePCR function in TBtools-II (Chen et al., 2023b) with TGERa-specific primers, we found that the A157 genome contains duplicated TGERa and TGERb loci arranged in a TGERb-TGERa -TGERb-TGERa pattern, which was inherited from its founder line PG6359 (Supplemental Table 4). Notably, the CDS of *TGERa*^{A157} and *TGERb*^{A157} are identical to those of *TGERa*^{E454} and *TGERb*^{E454}, respectively.

To identify the corresponding locus in A018, we sequenced, assembled, and annotated the A018 genome (Supplemental Figure 10; see Supplemental Note 2 for details). The predicted TGERa^{A018} protein shares 98.9% amino acid identity with TGERa^{E454}. We cloned the CDS of *TGERa*^{A018} and transiently expressed in *Nb* leaves. Similar to TGERa^{E454}, TGERa^{A018} induced MAPK activation and cell death upon Pep-13 treatment (Supplemental Figure 11A

346 and 11B), indicating that the TGERa^{A018} protein is functionally intact.
347 Using TBtools-II ePCR, we further identified the *TGERa* genomic sequence in
348 A018 genome and detected a ~3-kb insertion within the first intron of
349 *TGERa^{A018}* (Supplemental Figure 11C) and this insertion was also present in
350 the founder line PG6359 (Supplemental Table 4), leading us to hypothesize
351 that it might compromise *TGERa* expression in A018. Consistent with this
352 hypothesis, transcript analysis revealed that *TGERa* was strongly induced in
353 A157 following Pep-13 treatment, whereas only weak induction was observed
354 in A018 (Supplemental Figure 11D).
355 Considering that Pep-25 displays stronger cell-death-inducing activity than
356 Pep-13 (Supplemental Figure 3A), we further compared the response of A157,
357 A018, and Atlantic to both Pep-13 and Pep-25. As shown in Supplemental
358 Figure 11E and 11F, A157 exhibited robust cell death as early as 1 day after
359 infiltration with either Pep-25 or Pep-13. In contrast, Pep-25 triggered delayed
360 cell death in A018 at 2-3 days post-treatment, whereas Pep-13 failed to induce
361 visible cell death. Neither peptide elicited cell death in Atlantic. Collectively,
362 these results demonstrate that *TGERa^{A018}* represents a weak allele
363 characterized by diminished expression, most likely caused by the ~3-kb
364 insertion in its first intron.
365
366 **TGERa improves plant resistance to *Phytophthora* pathogens**
367 To assess the role of TGERa in resistance to *Phytophthora* pathogens,
368 detached leaves of *N. benthamiana* transiently expressing empty vector (EV),
369 *35S:TGERa*, or *35S:TGERb* were inoculated with *P. capsici* BYA5 and
370 incubated in the dark at 28 °C for 2 days; disease progression was then
371 imaged under UV light (Figure 4A). Quantification of diseased leaf areas
372 revealed that TGERa significantly enhanced resistance to *P. capsici* BYA5
373 compared with EV, whereas TGERb did not confer any detectable
374 improvement in disease resistance (Figure 4B).
375 To further confirm TGERa conferred enhanced *Phytophthora* resistance, we

challenged transgenic *np-TGERa N. benthamiana* lines with *P. infestans* 1306. Detached leaves from *np-TGERa Nb* lines (#1, #2, #3) and wild-type *Nb* plants were inoculated with *P. infestans* and incubated in the dark at 18 °C. Quantification of diseased areas showed significantly smaller lesions in *np-TGERa* lines than in WT (Figures 4C and 4D). Similarly, transgenic *np-TGERa* MicroTom plants exhibited significantly reduced disease symptoms relative to wild-type MicroTom at 2 days post-inoculation (Figures 4E and 4F). Collectively, these results demonstrated that introduction of *TGERa* into heterologous plant species significantly enhances resistance to *Phytophthora* pathogens.

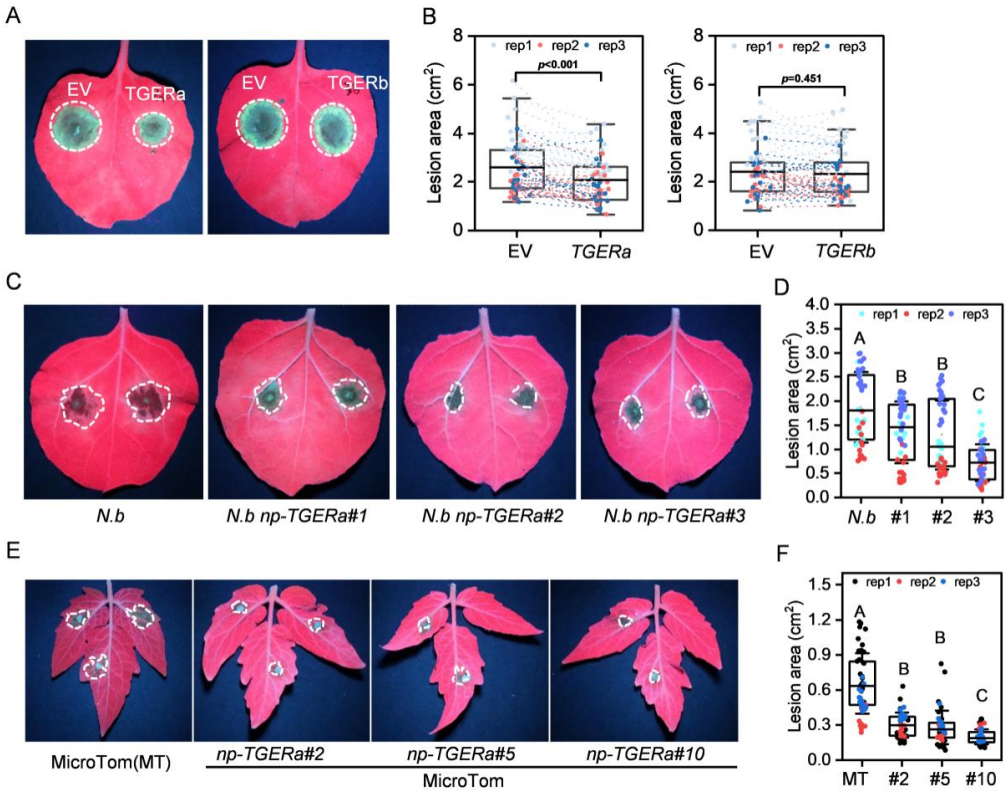

Figure 4. *TGERa* improves plant resistance to *Phytophthora*.

(A-B) *TGERa* enhances resistance to *Phytophthora capsici* when transiently expressed in *N. benthamiana* (*Nb*) leaves. **(A)** Empty vector (EV), *35S-TGERa* and *35S-TGERb* were transiently expressed in *Nb* leaves for 24 h, followed by inoculation with an agar plug (5 mm diameter from colony margins of *P. capsici* strain BYA5. Detached leaves were incubated in the dark at 28°C for 2 days, and lesions were photographed under UV light. **(B)** Quantification of lesion areas using ImageJ. Data were analysed using paired t-test (*TGERa*, $p < 0.05$, n=55 from three independent experiments; *TGERb*, $p = 0.451$, n = 56 from three independent experiments).

(C-D) Transgenic *Nb* lines expressing *TGERa* exhibit enhanced resistance to *P. infestans.* **(C)** Detached leaves of transgenic *Nb* lines (*np-TGERa* #1, *np-TGERa* #2, *np-TGERa* #3) and wild-type *Nb* plants were inoculated with *a* spore suspension of *P. infestans* strain 1306 and incubated in the dark at 18°C for 5 days and photographed under UV light. **(D)** Quantification of lesion areas using ImageJ. Data were analyzed using one-way ANOVA followed by Tukey's test. Different letters indicate significant differences ($p < 0.05$, n = 46 from three independent experiments).

(E-F) Transgenic tomato (MicroTom) lines expressing *TGERa* display enhanced resistance to *P. infestans.* **(E)** Detached leaves were inoculated with a spore suspension of *P. infestans* strain 1306, and lesion sizes were visualized 2 days post-inoculation under UV light. **(F)** Quantification of lesion areas using ImageJ. Data were analyzed using one-way ANOVA followed by Tukey's test. Different letters indicate significant differences ($p < 0.05$, n = 45 from three independent experiments).

METHODS

Plant materials and growth conditions

Tetraploid potato cultivar Atlantic and diploid inbred lines A018, E454, and A157 (Zhang et al., 2021) are maintained in the lab. Potato plants and transgenic lines were propagated on Murashige and Skoog (MS) medium in growth chambers under long-day conditions (16 h light at 23°C and 8 h dark at 22°C).

For genetic analysis, the Pep-13–insensitive line A018 (female parent) was artificially cross-pollinated with E454 (male parent) at anthesis to genetate F_1 hybrid progeny. The F_1 plants were subsequently self-pollinated to produce the F_2 population. For soil-grown seedlings, *in vitro*-cultured potato plants were grown on MS medium for 1 week then transferred to sterile soil and further cultivated for 14 days. *N. benthamiana* and *S. lycopersicum* MicroTom were directly seed-sown in soil composed of nutrient soil, vermiculite, and perlite (3:2:1, v/v/v). Plants were grown in a growth chamber under long-day conditions (16 h light at 23°C and 8 h dark at 22°C).

Peptide treatments

Peptides Pep-13 (VWNQPVRGFKVYE), Pep-13W2A (VANQPVRGFKVYE), and Pep-25 (DVTAGAEVWNQPVRGFKVYEQTKMS) (Brunner et al., 2002), Biotin-Pep-13, Biotin-Pep-25 and flg22 (QRLSTGSRINSAKDDAAGLQIA)

430 were synthesized by Sangon Biotech (Shanghai, China) Peptides were
431 dissolved in sterile double-distilled water (ddH_2O) to generate 2 mM stock
432 solutions and stored at -20°C. Working solutions were prepared by diluting
433 stock solutions with sterile water to indicated concentrations.

434 **Vector construction**

435 Primers used in this study are listed in Supplemental Table 6. Full-length
436 coding sequences of *TGERa*, *TGERb*, *StSERK1a*, *StSERK1b*, *StSERK2a*,
437 *StSERK2b*, *StSERK3a*, *StSERK3b* were cloned from cDNA library derived
438 from of E454 leaf. Domain swapping constructs between TGERa and TGERb
439 LRR regions were generated using gene-specific primers. PCR fragments
440 were inserted into pTF101-35S-3Flag vector (Bu et al., 2021) digested with
441 *XbaI* and *MluI* using homologous recombination. *StSERK1a*, *StSERK1b*,
442 *StSERK2a*, *StSERK2b*, *StSERK3a*, *StSERK3b* were inserted into
443 pCAMBIA1300-35S-3HA vector digested with HindIII and KpnI using
444 homologous recombination.

445 For virus-induced gene silencing constructs, TRV2-NbSERK conserved
446 regions (300-500 bp) within *SERK* coding sequences were identified by
447 BLAST analysis against the tobacco genome. Targeted fragments were
448 amplified and inserted into the TRV2 vector via homologous recombination. All
449 constructs were verified by Sanger sequencing.

450 ***Agrobacterium*-mediated transient expression**

451 Recombinant *Agrobacterium tumefaciens* strains GV3101 harboring the
452 indicated constructs were cultured overnight in LB medium supplemented with
453 kanamycin (50 μg/mL), rifampicin (25 μg/mL), and gentamycin (50 μg/mL) at
454 28 ℃ with shaking at 200 rpm. Bacterial cells were harvested by centrifuged at
455 5000 rpm for 5 min and washed twice with infiltration buffer conting10 mM
456 $MgCl_2$, 10 mM MES (pH 5.6), and 200 μM acetosyringone. Cells were
457 resuspended in infiltration buffer to a final OD_{600} of 0.6 and incubated at room
458 temperature in the dark for 3 h. Fully expanded leaves of 4–5-week-old *N.*
459 *benthamiana* plants were infiltrated on the abaxial side using a needleless

460 syringe. Plants were maintained under low light conditions for 24 h and then
461 returned to normal growth conditions. Protein expression was verified by
462 immunoblot analysis 24-48 h after infiltration. For elicitor assays, infiltration
463 sites were treated with 100 μM Pep-13 at 24 h post infiltration. Hypersensitive
464 cell death was evaluated 48 h later under 365 nm UV light.

465 **RNA isolation and RT-qPCR**

466 RNA isolation and RT-qPCR was performed as described (Chen et al., 2024).
467 *NbEF1α* was used as the reference gene for *N. benthamiana* samples, and
468 *StTUB* was used as the reference gene for potato (*S. tuberosum*). Relative
469 expression levels were calculated using the $2^{-\Delta\Delta CT}$ method. Primer sequences
470 are listed in Supplemental Table 6.

471 **MAPK activation assays**

472 Leaves of potato lines A018 and A157 were sprayed with 100 μM Pep-13, 5
473 μM flg22 or H_2O. Samples were collected at 15 and 30 min after treatment. *N.*
474 *benthamiana* leaves infiltrated with recombinant *Agrobacterium tumefaciens*
475 GV3101 as described previously for 24 hours, then infiltrated with 50 uM
476 peptides (Pep-13, Pep-25, W2A) for 15 min. Proteins were separated on 10%
477 SDS-PAGE and detected using anti-p44/42-ERK antibody (Cell Signaling
478 #9101).

479 **Virus-induced gene silencing (VIGS)**

480 Cotyledons of 2-week-old *N. benthamiana* plants or transgenic *np-TGERa*
481 lines were infiltrated with a 1:1 mixture of *Agrobacterium* cultures containing
482 pTRV1 and pTRV2 derivatives, *pTRV2-NbPDS*, *TRV2-GFP*, and
483 *pTRV2-NbSERKs* (Wang et al., 2018) adjusted to OD_{600} = 0.5. Two weeks
484 post-infiltration, plants showing photobleaching in *pTRV2-NbPDS*. Gene
485 silencing efficiency was confirmed by RT-qPCR. Leaves were then treated with
486 100 μM Pep-25 or H_2O and cell death responses were documented under 365
487 nm UV light 48 h later.

488 **Electrolyte leakage assay**

489 Electrolyte leakage assay was performed as reported (Fan et al., 2026). Briefly,

490 leaf discs (8 mm) were punched from peptide- or water-infiltrated leaves. Six
491 discs per replicate immersed in 2 mL deionized water. After 3 h incubation at
492 25 °C, initial conductivity (R1) was measured. Samples were boiled for 30 min,
493 cooled to 25 °C, and final conductivity (R2) recorded. Relative electrolyte
494 leakage (REL) was calculated as: REL (%) = (R1/R2) × 100%.

495 **Stable transformation of *N. benthamiana*, *Solanum tuberosum* (*cv.***
496 **Atlantic) and *S. lycopersicum* (*cv.* MicroTom)**

497 Stable transformation of *N. benthamiana*, MicroTom and Atlantic plants was
498 carried out by the BioRun company via *Agrobacterium*-mediated
499 transformation, using the construct *np-TGERa-3Flag* for *N. benthamiana* and
500 MicroTom, and the construct *35S-TGERa-3HA* for Atlantic. Transgenic plants
501 were screened by PCR using gene-specific primer to confirm the presence of
502 the *TGERa* transgene. TGERa protein levels in positive lines were further
503 verified by Western blot analysis.

504 ***In vivo* ligand binding assays**

505 *Agrobacterium tumefaciens* GV3101 carrying *TGERa-3flag* or *TGERb-3flag*
506 constructs was transiently expressed in *N. benthamiana* leaves for 24 h.
507 Leaves were then infiltrated with solutions containing 100 nM biotin–Pep-13/25
508 alone or together with 100 μM unlabeled Pep13/25 as a competition. The
509 infiltration buffer contained 3 mM ethylene glycol bis (succinimidyl succinate)
510 (EGS, Thermo Scientific, #21565) in 25 mM HEPES (pH 7.5). After 30 minutes,
511 approximately 1 g of leaf tissue was harvested and frozen in liquid nitrogen.
512 Proteins were immunoprecipitated using anti-Flag M2 affinity resin
513 (Sigma-Aldrich, A2220-5ML). Bound proteins were analyzed by
514 immunoblotting using anti-Flag antibody (Sigma-Aldrich, F1804-200UG) and
515 streptavidin-HRP (Abcam, Ab7403) to detect receptor-bound biotinylated
516 peptides.

517 **Co-immunoprecipitation assay**

518 Frozen leaf tissue was ground into a fine powder in liquid nitrogen and

519 homogenized in membrane extract buffer containing 25 mM Tris HCl (pH 7.5),
520 10% Glycerol, 1 mM EDTA, 150 mM NaCl, 1.5% NP-40, 0.5% sodium
521 deoxycholate, 1 mM NaF, 4 mM DTT, 2% (w/v) PVPP, 1 mM PMSF, and
522 protease cocktail. Protein extracts were incubated on ice for 30 min and
523 centrifuged at 13,000 × g for 15 min at 4 °C. The supernatants were clarified by
524 a second centrifugation under the same conditions. For immunoprecipitation,
525 the supernatants were incubated with 15 μL anti-FLAG M2 affinity resin
526 (Sigma-Aldrich, A2220-5ML) for 2 h at 4 °C with gentle rotation. Input samples
527 were retained for immunoblot analysis. The resin was washed three times with
528 binding buffer containing 25 mM Tris HCl (pH 7.5), 10% Glycerol, 1 mM EDTA,
529 150 mM NaCl, 1.5% NP-40, 0.5% sodium deoxycholate, 1 mM NaF, 0.2 mM
530 DTT. Bound proteins were eluted by boiling in 2× SDS loading buffer at 95 °C
531 for 5 min. Proteins were separated by SDS–PAGE and detected by
532 immunoblotting using anti-Flag and anti-HA antibodies.

533 **Interacting proteins identified by Immunoprecipitation-Mass**
534 **Spectrometry（IP-MS）**

535 *TGERa-3Flag* or empty vector (EV) constructs were transiently expressed in *N.*
536 *benthamiana* leaves. At 48 h after agroinfiltration, leaves were treated with 100
537 μM Pep-13 or H_2O and harvested 15 min after treatment. Total proteins were
538 extracted and subjected to immunoprecipitation using anti-FLAG M2 affinity
539 resin as described above. Immunoprecipitated proteins were separated by
540 SDS-PAGE and visualized by Coomassie Brilliant Blue staining. Gel regions
541 containing TGERa protein complex were excised and subjected to in-gel
542 digestion with tryptic.

543 The resulting peptides were analyzed by liquid chromatography-tandem mass
544 spectrometry (LC-MS/MS) using an EASY-nLC 1200 system coupled to an
545 Orbitrap Exploris 480 mass spectrometer (Thermo Fisher Scientific). Peptides
546 were separated on a C18 analytical column using a linear acetonitrile gradient.
547 Raw MS data were processed using Proteome Discoverer software and

548 searched against the NbHZ1 protein database (Wang et al., 2024).
549 Carbamidomethylation of cysteine residues was set as a fixed modification,
550 whereas methionine oxidation was considered a variable modification. Up to
551 two missed trypsin cleavage sites were allowed. Peptide spectrum matches
552 were filtered using a false discovery rate (FDR) threshold of <1%. Functional
553 annotation of identified proteins was performed using Gene Ontology (GO),
554 InterPro, COG, and KEGG databases. Only proteins identified in at least two
555 biological replicates were considered for further analysis.

556 **Luminol-based ROS burst assay**

557 Leaf discs (4 mm diameter) were excised from 5-week-old *N. benthamiana*
558 plants were equilibrated overnight in 200 μL ddH_2O in 96-well white plates. The
559 next day, water was replaced with 100 μL reaction buffer containing 10 μg/mL
560 horseradish peroxidase (HRP; Sigma #P6782), 50 μM luminol (Sigma #A8511),
561 and 50 nM Pep-13. Real-time luminescence was recorded at 1 min intervals
562 for 120 min using a Cytation5 microplate reader (BioTek, Winooski, VT, USA)
563 with the following parameters: gain 130, 5 mm read height, no optical filter, and
564 maintaining a constant temperature of 22 °C.

565 **Pathogen infection assay**

566 Infection assays were performed as described previously (Chen et al., 2024). *P.*
567 *infestans* strain 1306 was cultured on rye agar medium at 18 ℃ in darkness for
568 14 days. Zoospores were released by incubating sporangia in cold water at
569 4 °C for 2 h and filtered to remove mycelium. Detached leaves were inoculated
570 with 5 μL zoospore suspension (1×10^5 spores/mL) on the abaxial surface.
571 For *P. capsica* strain BYA5 (Gao et al., 2023), clones were cultured on V8 juice
572 agar medium at 25 ℃ in darkness for 3 days. Agar plugs (5 mm diameter) from
573 colony margins were placed onto leaf surface and covered with 10 μL sterile
574 water. Infected leaves were incubated under 100% relative humidity at optimal
575 temperatures (18 °C for *P. infestans*, 25 °C for *P. capsica*) for 4 or 3 days,
576 respectively. Lesion areas were visualized under UV light and quantified using
577 ImageJ (v1.51j8, National Institutes of Health, Maryland, USA) software.

578 **Statistical Analysis**

579 All experiments were performed with at least three independent biological
580 replicates unless otherwise stated. Data are presented as mean ± standard
581 deviation (SD). Statistical analyses were performed using OriginPro2025
582 (OriginLab). Statistical significance between two groups was determined using
583 a two-tailed Student's t-test, while comparisons among multiple groups were
584 analyzed using one-way analysis of variance (ANOVA) followed by Tukey's
585 multiple comparison test. Differences were considered statistically significant
586 at $p < 0.05$.

587 **DATA AVAILABILITY**

588 The authors hereby declare that all relevant data supporting the findings of this
589 study are accessible within the research article and its supplemental
590 information. The A018 genome data has been deposited at
591 http://solomics.agis.org.cn/potato/species, under Accession A6-10 (A018).
592 Materials generated during the current study are available from the
593 corresponding author upon reasonable request.

594 **FUNDING**

595 The research was supported by grants from the AGIS Talents Start-up
596 Research Fund, Agricultural Science and Technology Innovation Program,
597 Guangdong Basic and Applied Basic Research Foundation
598 (2024A1515010069), and National Natural Science Foundation of China
599 (General Program, 32472579) to TS.

600 **ACKNOWLEDGMENTS**

601 We thank Yan Wang from Nanjing Agricultural University for kindly sharing
602 pTRV2-NbSERKs, and Fanjiang Kong from Guangzhou University for kindly
603 sharing pTF101-35S-3FLAG vector. We thank Suomeng Dong from Nanjing
604 Agricultural University for kindly providing the *Phytophthora infestans* strain
605 1306. We also thank Xili Liu from Northwest A&F University for generously
606 providing the *Phytophthora capsici* strain BYA5 and the pMDC vector. We
607 thank the members of our research group for their technical assistance and

helpful suggestions. The authors declare no conflicts of interest.

AUTHOR CONTRIBUTIONS

T.S., X.F., D.L., and L.C. conceived and designed this study; C.Z., and S.H. provided advice and initial materials; X.F., D.L., Y.Z., and Y.H. performed the experiments; L. C. analyzed BSA-seq data and performed assemble and annotation of A018 genome. T.S., X.F., and L.C. wrote the manuscript from the input from all other authors. All authors reviewed the manuscript.

SUPPLEMENTAL INFORMATION

Supplemental information is available online.

Supplemental Note 1. Mapping the TGER locus by BSA-seq analysis.
Supplemental Note 2. A018 genome assembly and annotation.
Supplemental Figure 1. Mapping of *TGER* locus using bulked segregant analysis sequencing
Supplemental Figure 2. Transient expression of selected candidate genes in *N. benthamiana* leaves by *Agrobacterium* and tested for responding to Pep-13.
Supplemental Figure 3. Functional confirmation of TGERa by transgenic complementation.
Supplemental Figure 4. Identification of six NbSERK proteins as Pep-13 induced interacting proteins of TGERa by IP-MS and phylogenetic analysis of SERK proteins.
Supplemental Figure 5. TGERa relies on SERKs for Pep-13 perception.
Supplemental Figure 6. Translation initiation from uORF1 of TGERa mRNA leads to decreased TGERa protein levels.
Supplemental Figure 7. Intron 2 retention is observed in a subset of TGERa/PERU transcripts.
Supplemental Figure 8. The TGERa protein (TGERa-In2R) translated from TGERa mRNA with intron 2 retention cannot recognize Pep-13/25.
Supplemental Figure 9. Functional characterization of TGERb in Pep-13 perception and signaling.
Supplemental Figure 10. Genome assembly and annotation of potato inbred line A018.
Supplemental Figure 11. TGERa in A018 is a weak allele with reduced expression.
Supplemental Table 1. 1,981 candidate variants on Chr03 of E454 genome identified by BSA-seq analysis.
Supplemental Table 2. SNPs identified in selected 24 candidate genes.
Supplemental Table 3. Selected candidate genes and cloning primers used.

647 Supplemental Table 4. ipTM between Pep-13 and ectodomains of TGERa,
648 TGERb and TGERa variants predicted using AlphaFold3.
649 Supplemental Table 5. ePCR results for TGER primers in genomes of A018,
650 A157, E454, E86-69, PG6359, DM and Atlantic.
651 Supplemental Table 6. Primers used in this study.
652

653 **REFERENCES**

654 **Albert, I., Böhm, H., Albert, M., Feiler, C. E., Imkampe, J., Wallmeroth, N., Brancato, C.,**
655 **Raaymakers, T. M., Oome, S., Zhang, H., et al.** (2015). An RLP23-SOBIR1-BAK1
656 complex mediates NLP-triggered immunity. *Nat. Plants* **1**:1–9.

657 **Brunner, Â., Rosahl, S., Lee, J., Rudd, J. J., Geiler, C., Scheel, D., and Nu, T.** (2002).
658 Pep-13, a plant defense-inducing pathogen-associated pattern from phytophthora
659 transglutaminases. *EMBO J.* **21**:6681–6688.

660 **Bu, T., Lu, S., Wang, K., Dong, L., Li, S., Xie, Q., Xu, X., Cheng, Q., Chen, L., Fang, C., et**
661 **al.** (2021). A critical role of the soybean evening complex in the control of photoperiod
662 sensitivity and adaptation. *Proc. Natl. Acad. Sci. U. S. A.* **118**:1–10.

663 **Chen, Z., Liu, F., Zeng, M., Wang, L., Liu, H., Sun, Y., Wang, L., Zhang, Z., Chen, Z., Xu, Y.,**
664 **et al.** (2023a). Convergent evolution of immune receptors underpins distinct elicitin
665 recognition in closely related Solanaceous plants. *Plant Cell* Advance Access published
666 2023, doi:10.1093/plcell/koad002.

667 **Chen, C., Wu, Y., Li, J., Wang, X., Zeng, Z., Xu, J., Liu, Y., Feng, J., Chen, H., He, Y., et al.**
668 (2023b). TBtools-II: A “one for all, all for one” bioinformatics platform for biological
669 big-data mining. *Mol. Plant* Advance Access published 2023,
670 doi:10.1016/j.molp.2023.09.010.

671 **Chen, Y., Han, Y., Huang, W., Zhang, Y., Chen, X., Li, D., Hong, Y., Gao, H., Zhang, K.,**
672 **Zhang, Y., et al.** (2024). LAZARUS 1 functions as a positive regulator of plant immunity
673 and systemic acquired resistance. *Front. Plant Sci.* **15**:1–11.

674 **Cheng, L., Wang, N., Bao, Z., Zhou, Q., Guarracino, A., Yang, Y., Wang, P., Zhang, Z.,**
675 **Tang, D., Zhang, P., et al.** (2025). Leveraging a phased pangenome for haplotype
676 design of hybrid potato. *Nature* **640**:408–417.

677 **Du, J., Verzaux, E., Chaparro-Garcia, A., Bijsterbosch, G., Keizer, L. C. P., Zhou, J.,**
678 **Liebrand, T. W. H., Xie, C., Govers, F., Robatzek, S., et al.** (2015). Elicitin recognition

679 confers enhanced resistance to Phytophthora infestans in potato. *Nat. Plants* **1**:15034.
680 **Fan, X., Han, Y., Sun, X., and Sun, T.** (2026). Identification and Functional Analysis of Potato
681 Receptor Kinase RDA2 Proteins. *Plants* **15：1-14**.
682 **Gao, H., Guo, Y., Ren, M., Tang, L., Gao, W., Tian, S., Shao, G., Peng, Q., Gu, B., Miao, J.,**
683 **et al.** (2023). Phytophthora RxLR effector PcSnel4B promotes degradation of resistance
684 protein AtRPS2. *Plant Physiol.* **193**:1547–1560.
685 **Jones, J. D., and Dangl, J. L.** (2006). The plant immune system. *Nature* **444**:323–329.
686 **Li, Y., Tao, Y., Yao, X., Cao, R., Xiong, X., Gong, B.-Q., and Li, J.-F.** (2025). SERK5
687 genetically compensates for the loss of BAK1 and BKK1 in regulating elf18-triggered
688 immune signaling in *Arabidopsis*. *Proc. Natl. Acad. Sci.* **122**:e2513517122.
689 **Ma, X., Xu, G., He, P., and Shan, L.** (2016). SERKing Coreceptors for Receptors. *Trends*
690 *Plant Sci.* **21**:1017–1033.
691 **Nietzschmann, L., Gorzolka, K., Smolka, U., Matern, A., Eschen-Lippold, L., Scheel, D.,**
692 **and Rosahl, S.** (2019). Early Pep-13-induced immune responses are
693 SERK3A/B-dependent in potato. *Sci. Rep.* **9**:1–12.
694 **Nowicki, M., Foolad, M. R., Nowakowska, M., and Kozik, E. U.** (2012). Potato and Tomato
695 Late Blight Caused by Phytophthora infestans：An Overview of Pathology and
696 Resistance Breeding. *Plant Dis.* **96**:4–17.
697 **Nürnberger, T., Nennstiel, D., Jabs, T., Sacks, W. R., Hahlbrock, K., and Scheel, D.** (1994).
698 High affinity binding of a fungal oligopeptide elicitor to parsley plasma membranes
699 triggers multiple defense responses. *Cell* **78**:449–460.
700 **Stokstad, E.** (2019). The new potato. *Science (80-.).* **363**:574–577.
701 **Torres Ascurra, Y. C., Zhang, L., Toghani, A., Hua, C., Rangegowda, N. J., Posbeyikian,**
702 **A., Pai, H., Lin, X., Wolters, P. J., Wouters, D., et al.** (2023). Functional diversification
703 of a wild potato immune receptor at its center of origin. *Science (80-.).* **381**:891–897.
704 **Wang, Y., Xu, Y., Sun, Y., Wang, H., Qi, J., Wan, B., Ye, W., Lin, Y., Shao, Y., Dong, S., et**
705 **al.** (2018). Leucine-rich repeat receptor-like gene screen reveals that Nicotiana RXEG1
706 regulates glycoside hydrolase 12 MAMP detection. *Nat. Commun.* **9**.
707 **Wang, J., Zhang, Q., Tung, J., Zhang, X., Liu, D., Deng, Y., Tian, Z., Chen, H., Wang, T.,**
708 **Yin, W., et al.** (2024). High-quality assembled and annotated genomes of Nicotiana

709 tabacum and Nicotiana benthamiana reveal chromosome evolution and changes in
710 defense arsenals. *Mol. Plant* **17**:423–437.
711 **Zhang, C., Yang, Z., Tang, D., Zhu, Y., Wang, P., Li, D., Zhu, G., Xiong, X., Shang, Y., Li,**
712 **C., et al.** (2021). Genome design of hybrid potato. *Cell* **184**:3873-3883.e12.
713 **Zhou, J., and Zhang, Y.** (2020). Plant Immunity: Danger Perception and Signaling. *Cell*
714 **181**:978–989.
715